

# Prediction of Acoustic Loads Generated by Propulsion Systems

Linamaria Perez<sup>1</sup>

*University of Puerto Rico Mayagüez Campus, Mayagüez, PR, 00680*

Daniel C. Allgood<sup>2</sup>

*NASA-Stennis Space Center, Stennis Space Center, MS 39529*

NASA Stennis Space Center is one of the nation's premier facilities for conducting large-scale rocket engine testing. As liquid rocket engines vary in size, so do the acoustic loads that they produce. When these acoustic loads reach very high levels they may cause damages both to humans and to actual structures surrounding the testing area. To prevent these damages, prediction tools are used to estimate the spectral content and levels of the acoustics being generated by the rocket engine plumes and model their propagation through the surrounding atmosphere. Prior to the current work, two different acoustic prediction tools were being implemented at Stennis Space Center, each having their own advantages and disadvantages depending on the application. Therefore, a new prediction tool was created, using NASA SP-8072 handbook as a guide, which would replicate the same prediction methods as the previous codes, but eliminate any of the drawbacks the individual codes had. Aside from replicating the previous modeling capability in a single framework, additional modeling functions were added thereby expanding the current modeling capability. To verify that the new code could reproduce the same predictions as the previous codes, two verification test cases were defined. These verification test cases also served as validation cases as the predicted results were compared to actual test data.

## Nomenclature

$a_{cl}$	=	classical losses, dB
$a_e$	=	speed of sound in the flow at the nozzle exit, m/sec
$a_{max}$	=	maximum molecular absorption due to the vibrational mode
$a_o$	=	speed of sound in the atmosphere, m/sec
$a'_{mol}$	=	molecular absorption losses, dB
$d, D$	=	diameter
$f$	=	frequency, Hz
$f_m$	=	frequency of maximum absorption per wavelength
$h$	=	percent mole ratio
$h'$	=	absolute humidity, gm/m <sup>3</sup>
$M_e$	=	exit Mach number
$P^*$	=	pressure relative to 14.7 psi
$SPL$	=	Sound Pressure Level
$T^*$	=	absolute temperature relative to 519°R
$U_e$	=	exit velocity
$W$	=	acoustic power
$W_{OA}$	=	overall acoustic power
$x$	=	distance along plume
$x_c$	=	core length

## I. Introduction

Rocket engines come in all types of sizes and the higher the thrust of the engine the more acoustic loads it will produce. At a testing facility different sized engines are tested and if the engines generate acoustic levels that are too

<sup>1</sup> Student Department of Mechanical Engineering, Stennis Space Center, University of Puerto Rico Mayagüez Campus

<sup>2</sup> Engineer, NASA Stennis Space Center, Design and Analysis Group, Bldg. 3225 Stennis Space Center, MS 39529

high they can cause structural damage from vibration or even cause damage to the human ear from the loudness. Therefore, it is important to be able to predict the acoustic levels for the different types of engines before the actual tests can be conducted. At NASA Stennis Space Center (SSC), two types of prediction tools were used to calculate the acoustic loads, a code that runs on MathCad and a code that runs on Fortran. Although these tools are able to make the predictions, they had their downsides of either running too slow or not being able to be used for certain analyses. Working off of these limitations a new prediction tool was created - a Matlab code that would combine unique features from each of the previous codes and have other functions added on to them as well. The NASA SP-8072 handbook was used as a guide to make all the calculations necessary to obtain the overall sound pressure levels which allow us to see the decibel levels of the acoustic loads generated.

## II. Acoustics

Acoustics is the science that focuses on the study of mechanical waves in solids, liquids, and gases. This includes sound, vibration, ultrasound, and infrasound. The physical process is that a noise source generates the sound waves that will propagate through the air. As these sound waves propagate they create pressure changes in the air which can be sensed by the human ear or by microphones. These sound waves that travel through the air vary in frequency, which is the number of cycles the wave completes per second. Some may be high frequency sound waves, which are many cycles per second, and others can be low frequency, which are a small number of cycles per second. The loudness or strength of the sound waves is generally characterized by a sound pressure level (units of decibels), which is a logarithmic representation of the pressure fluctuations normalized in respect to a reference pressure. The reference pressure is typically  $20 \times 10^{-6}$  Pa. Ultimately, the objective in an acoustic prediction process is the quantification of the sound pressure levels for each significant acoustic wavelength being generated and the subsequent attenuation or amplification of these waves as they propagate through the surrounding environment.

## III. Jet Noise

The primary noise source during rocket engine testing is the jet noise generated by the rocket exhaust plume. The jet noise is produced directly from the formation, propagation and dissipation of vortices or eddies that are formed in the shear layer of the plume. These eddies are very small in size near the nozzle exit where they originally form and as they propagate along the plume they become larger until they eventually dissipate. Once the sound waves that are created from the eddies begin to propagate through the air and spread out over an area they create pressure changes that will then be picked up by the microphones. Since these sound waves vary in frequency, a spectrum of varying sound pressure levels will be generated along the length of the plume. Figure 1 depicts the propagation of the sound waves from the plume boundary and the relative changes in spectral content as would be seen by an observer moving along the plume.

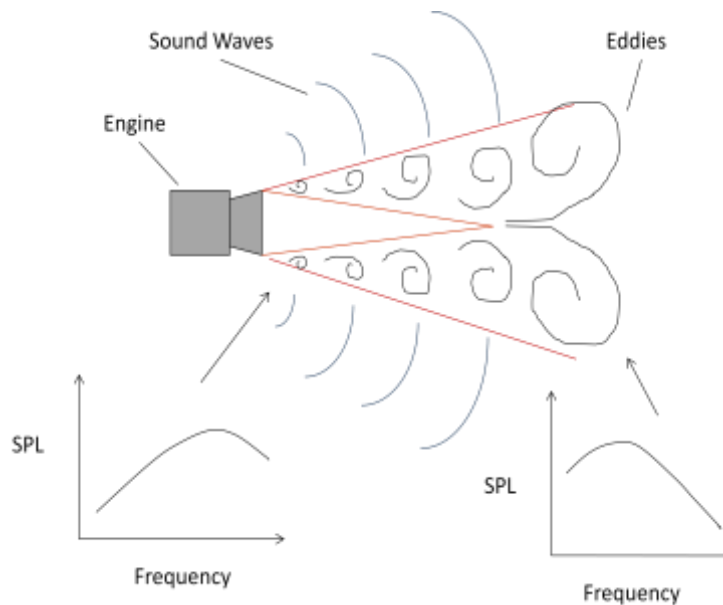


Figure 1. Sound Wave Propagation

#### IV. Similarity in Rocket Engine Acoustics

##### A. Spectra of Overall Sound Power Levels

Each rocket engine generates its own unique acoustic spectra due to variations in size, thrust levels, propellants being used, etc. However, by appropriately non-dimensionalizing acoustic data obtained during rocket engine testing, dynamic similarity has been observed. To accomplish the normalization of the data, the Strouhal number is introduced, which takes the frequency and multiplies it times the rocket nozzle exit diameter and divides it by the fully expanded exit velocity. A perfect example is shown in Fig. 2, taken from the NASA SP-8072 handbook. This figure shows how sound power-level spectra for different types of engines have been effectively reduced to a single acoustic spectrum. The resulting non-dimensional relation can then be used to predict acoustical environments generated by a wide range of engines.

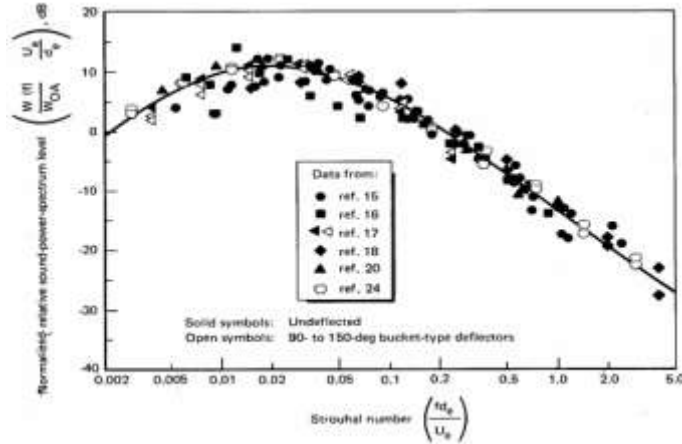


Figure 2. Sound Power Level Spectrum versus Frequency [1]

##### B. Directivity of Acoustic Levels

Another important concept in modeling rocket engine acoustics is the directivity at which the sound propagates. The sound waves do not propagate uniformly in all directions due to refraction by the rocket exhaust plume. The amount in which the overall sound pressure levels will be refracted depends on the type of engine as it is directly affected by the temperature of the exhaust exiting from the nozzle. The hotter the exhaust the more the sound will be radiated outward away from the axis of the jet as depicted in Fig. 3. Thus, when performing an acoustic analysis, the sound pressure levels must be corrected based on the relative angle of the observer to the plume axis. This correction is typically defined as the directivity index, which has been shown to be dependent on both angle and frequency. As was seen with the spectra of the sound power levels, the dependency on frequency can be normalized using the Strouhal number. Figure 4 provides the directivity curves used for standard chemical rockets as suggested by NASA SP-8072. The figure indicates that the amount of refraction increases with Strouhal number (or frequency) as the shorter acoustic wavelengths are more easily refracted by the plume. In an acoustic prediction, the directivity index data from this curve can be interpolated based on angle and Strouhal number in order to appropriately correct the sound pressure levels.

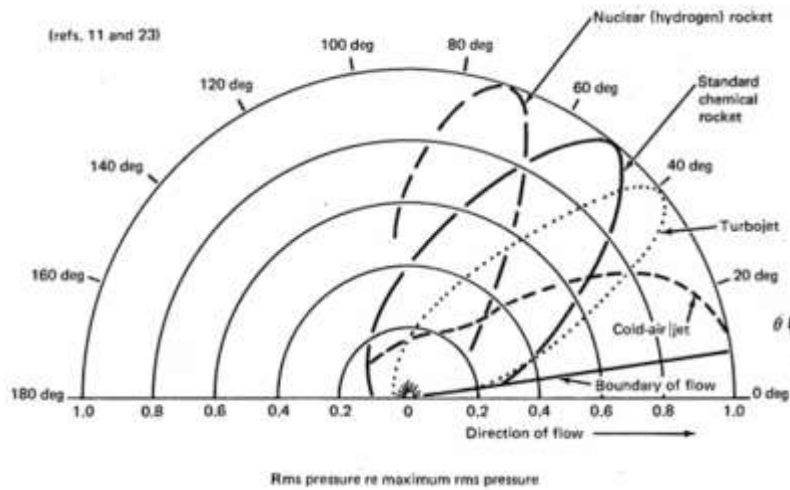


Figure 3. Directional Characteristics of Overall Sound Power Levels [1]

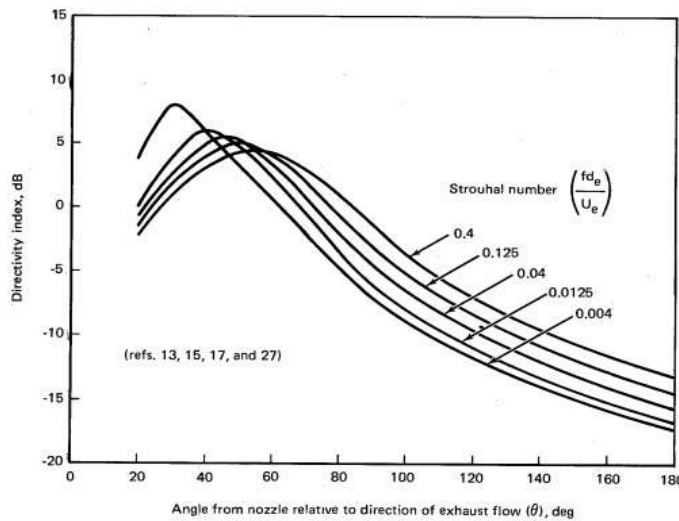


Figure 4. Directivity Index Curves [1]

### V. NASA SP-8072: Acoustic Loads Generated by the Propulsion Systems

Using the concept of dynamic similarity in rocket engine acoustics, the NASA SP-8072 handbook has established a few guidelines for predicting the acoustic environments generated by rocket engine plumes. There are three main empirical-based methods that can be used to make the predictions: point source method, first source-allocation method, and second source-allocation method. The point-source method can only be used to make predictions in the acoustic far-field while the first and second source allocation methods are valid in the near and far-fields. The main difference between near field and far field is that in the near field the acoustics behaves nonlinearly while in the far field it behaves linearly. Generally speaking, a point of interest which is a distance from the source of more than 100 to 200 nozzle exit diameters is considered as far-field. The philosophy behind each modeling method will now be discussed in detail.

#### A. Point Source Method

The point source method treats the acoustics generated by the rocket exhaust plume as being generated from a single point in space, namely the exit of the engine. The single noise source is characterized using the dynamic

similarity methods discussed in the previous section of this report and then the spreading of the acoustics to the surroundings is computed. The prediction is begun by determining the mechanical power of the engine using the engine thrust and nozzle exit velocity. From this value and an estimate of the acoustic efficiency, which is the efficiency in which mechanical power is converted into acoustic power, the overall sound power level of the noise source (measured in decibels) can be computed. After obtaining this value, a conventional acoustic bandwidth is chosen, whether it is one octave or one third octave. These octaves will give the user the frequency bands that will be used in calculating the Strouhal number. Referring back to Fig. 2, which shows the normalized sound power levels versus Strouhal number, this spectrum is used to obtain the values of the sound power levels for each one of the frequency bands selected. Like the curve in Fig. 2 there are also other curves the user can select for ultra-high velocity rocket plumes (>8600 ft/sec) which characteristically have a slower low frequency roll-off in acoustic power. Once the sound power levels are obtained, the radial distance and angle of the point-of-interest in relation to the noise source and the plume axis are computed. The angle will be used along with the Strouhal number to calculate the directivity index for each angle along each frequency. With the sound power level, radial distance between the noise source and microphone, and the directivity indexes having been computed, the sound pressure level spectra and overall sound pressure level can then be determined. As mentioned before, these sound pressure levels, dB, are what is needed to measure the loudness of the noise generated from the engine. If the decibel levels are too high proper precautions can be taken to prevent any types of damage.

**B. First Source Allocation Method**

The first source allocation method follows the same general steps as the point source method to obtain the normalized sound power level spectra only this time the sound power level spectral bands are moved to specific locations along the axis of the plume thereby distributing the noise source over a finite length. The manner in which the frequencies are moved along the plume axis is according to the similarity curves of Fig. 5. The Strouhal numbers that were previously calculated are interpolated with the values from this figure to obtain the apparent source axial positions. This takes each tone from the original spectrum created at the exit of the nozzle and gives it a new location along the plume; hence the reason why it is considered a distributed method. However, in liquid rocket engine testing the plume is commonly redirected by a deflector which has either open or closed side-walls. Figure 5 provides correction terms for the apparent source locations for these applications. The values obtained from Fig. 5 are normalized values and must be multiplied by the nozzle exit diameter in order to determine the actual distance along the axis where the monotone noise sources should be placed. Using these distributed source locations, the radial distance and angles between the sources and points of interest needed in the acoustic propagation calculations can then be determined. The remaining calculations are computed in the same way to finally obtain the sound pressure levels needed for the predictions.

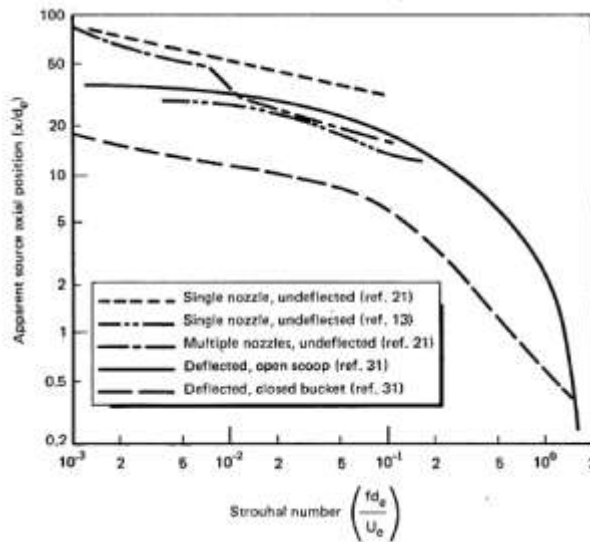
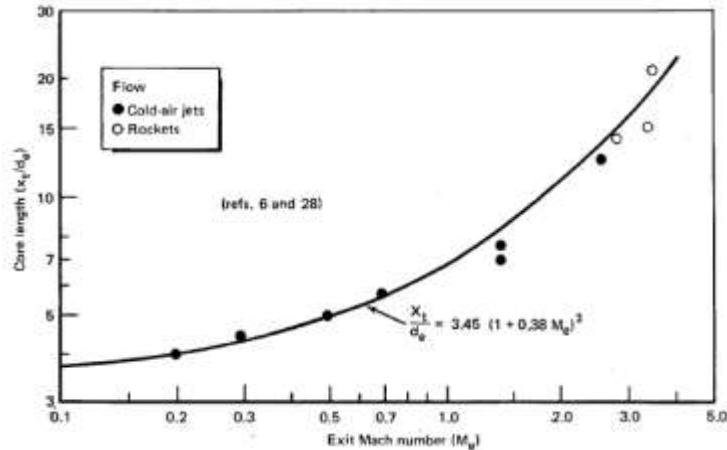


Figure 5. Apparent Source Locations [1]

**C. Second Source Allocation Method**

The second source allocation method introduces the concept of the laminar core length of the plume. The laminar core is the internal region of the plume where the flow is almost completely laminar. For an undeflected plume, the core extends from the nozzle exit to the point where the shear-layer intercepts the plume axis. The core length has been shown to be a function of primarily the engine exit Mach number, where Mach number is the ratio of exit velocity to speed of sound in the plume. Typically, the maximum sound power levels occur near the end of the laminar core region where the turbulence levels get amplified due to collision of unsteady flow structures at the plume axis. Figure 6 shows a relationship between the Mach number and the core length as recommended in SP-8072. This is one example of an empirical-based curve which can be used to determine the core length. However, the Varnier equation was proposed by Haynes et al [6] as a more accurate representation of rocket engine core length dependence on Mach number.

In the previous distributed method, the plume axis was defined along one direction and did not change. In applications where the engine is mounted on a vertical test stand, the plume does not follow a straight path and is redirected by the deflector. Thus, its noise source distribution is highly dependent on the shape of the deflector. It has been suggested in Ref. 6 that the core length be truncated to the distance between the nozzle exit and the point of impingement since a “laminar” core will no longer exist in the plume once it impinges on the deflector.



**Figure 6. Determining Core Length [1]**

Once the core length of the rocket plume is defined, the plume must be divided into slices. The number of slices will be determined by the user. As depicted in Fig. 7, the centers of each slice will be locations of individual noise sources. The location of the slices along the plume axis and the distribution of sound power level for each slice will be determined using the normalized data in Fig. 8. The fundamental difference between the first and second source allocation methods is that instead of treating the noise source as a distribution of single frequency tones as was done in the first allocation method, each slice has its own noise level spectrum. Figure 9 is the spectrum used to obtain the values for the normalized sound power levels. The Strouhal number has now been modified to include the location for each center of each slice and the speed of sound both in the atmosphere,  $a_o$ , and nozzle exit,  $a_e$ . With the normalized values for the sound power levels being determined for each slice of the plume, the remaining calculations remain the same as the previous methods with the equations now accounting for the additional noise sources.

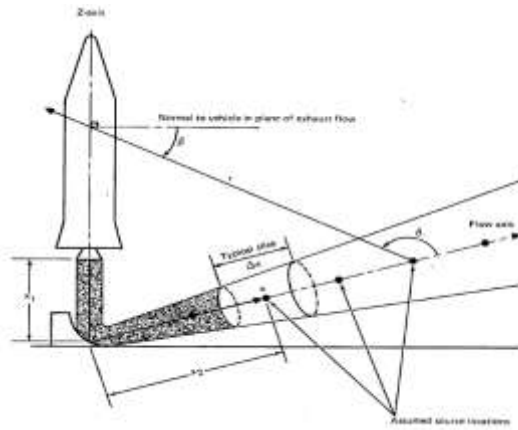


Figure 7. Dividing Plume into Slices [1]

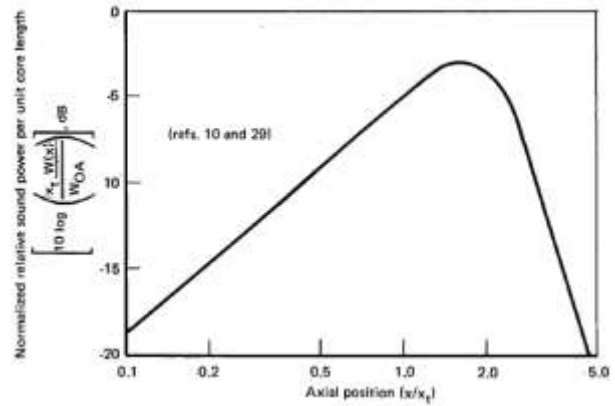


Figure 8. Normalized Sound Power Unit per Core Length versus Axial Position [1]

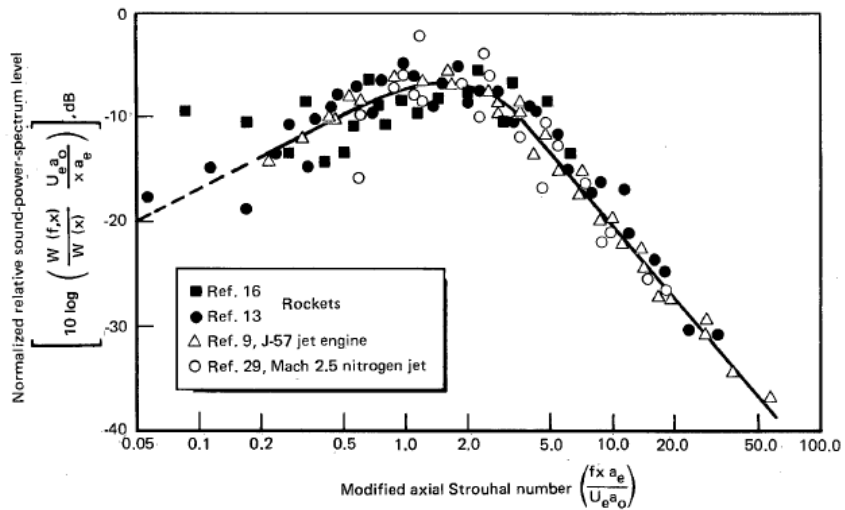


Figure 9. Normalized Sound Power Level versus Modified Strouhal number [1]

## VI. Previously Existing Acoustic Prediction Tools at Stennis Space Center

Stennis Space Center had two different prediction tools that were used for the predictions of the acoustic loads generated by propulsion systems. The codes made the predictions using the steps provided by the NASA SP-8072 handbook for different prediction methods. Each had their pros and their cons.

### A. MathCad SP-8072 Code

The first prediction tool was written in the MathCad programming language. The methodology that was used in the MathCad code was the first source allocation method only. While the MathCad code was able to make the predictions for the near and far-field analyses, it was limited in that it was restricted to only the directivity and spectra as provided in the SP-8072 manual. For certain deflected rocket plumes, it has been found that the directivity index provided by SP-8072 is not optimum. Rather, it is best to use custom directivity indexes derived from acoustic data for that particular test stand.

In addition to the lack of custom directivity data in this code, it would have been difficult to efficiently program the second source allocation method. Lastly, MathCad is notoriously slow in computation and displaying of the results. So it is not a tool that lends itself well to parametric studies.

**B. FORTRAN Point-Source Code**

The second prediction tool that was being used at Stennis Space Center was a code written in FORTRAN. The prediction method used in this code was the point source method. Again, the point source method only works well for analysis in the far-field as the points of interest are sufficiently far from the plume that the noise sources “appear” to be originating from a single source rather than a distribution of sources along the plume. Therefore, this program could not be used to make accurate near-field predictions. However, unlike the MathCad code described above, the FORTRAN code does have custom directivity index data which allows the user to pick the data that best fits the application. In addition, the FORTRAN code allowed for fast turn-around of parametric studies.

**VII. New Acoustic Prediction Tool - ALGPS**

**A. Overview of ALGPS**

Due to the benefits and limitations of each of the respective codes, it was desirable to combine the functionality of both codes into a single modeling frame work in order to make predictions for both near and far-field acoustics. Also, none of the existing codes had the function for the second source allocation method, which presumably allows for a more accurate prediction since the distributed sources in the plume are not monotone. Using the NASA SP-8072 manual as a guide, a brand new prediction tool (ALGPS) was created that would combine all the functions of the previous codes and implement the second source allocation method. ALGPS is an acronym which stands for Acoustic Loads Generated by Propulsion Systems, which was derived from the title of NASA SP-8072. ALGPS was written using the Matlab programming language.

To further improve the predictions for far-field acoustics, functions were built in to compute any losses that the sound waves might experience while propagating through the air. The ALGPS code has the capability to calculate classical losses and molecular losses due to the air itself. The losses can be quite significant for far-field propagation and therefore it is necessary to include their effects in making accurate predictions.

Another feature that was added to the new prediction tool was an option for modeling either spherical or hemispherical propagation. The previously existing MathCad code made predictions for spherical propagation only. Spherical propagation is used when an engine is being tested in a distance high enough off the ground that will allow the sound waves to propagate freely. However, for the majority of the rocket engine testing spherical propagation does not occur due to ground plane interference. To account for the engine being close to the ground, the hemispherical function is computed instead. ALGPS provides the option of deciding which type of propagation best represents the application of interest.

**B. Atmospheric Attenuation in ALGPS**

All sonic disturbances lose energy when propagating through the air due to the acoustic energy turning into heat energy. This process is irreversible and not accounting for these losses will result in inaccurate predictions. The NASA SP-8072 handbook does not provide any guidance on computing the losses due to propagation of the sound waves through the atmosphere. Two types of atmospheric losses were added to the new prediction tool - namely classical and molecular absorption losses. The equations for these losses were obtained from Ref. 2.

**1. Classical Losses**

Classical losses are inherent in all gases due to basic gas transport phenomena. When computing the classical losses you will notice that the units will be in decibels per 1,000 feet. The classical losses are very insignificant for small distances and the noticeable differences will only occur at distances greater than 1,000 feet. Equation (1) was the equation selected to compute the classical losses. It is dependent on frequency only.

$$a_{cl} = 5.3 \times 10^{-8} f^2; \frac{dB}{1000} ft \tag{1}$$

**2. Molecular Losses**

Molecular losses are due to the resonance phenomena within polyatomic gases and losses due to radiation of heat energy. The molecular losses are very dependent on its surroundings. Many derivations of the molecular loss equation have been made as well as corrections. Equation (2) shows the final equation that was used, after all derivations and corrections were made.

$$a'_{mol} = a_{max} \left\{ \left[ \frac{0.18 f}{f_m} \right]^2 + \left[ \frac{2(f/f_m)^2}{1+(f/f_m)^2} \right]^2 \right\}^{1/2} \quad (2)$$

$$a_{max} = 0.0078 f_m (T^*)^{-2.5} e^{7.77(1-1/T^*)} \quad (3)$$

$$f_m = (10 + 6600h + 44,400 h^2)(P^*/T^*)^{0.8}; Hz \quad (4)$$

$$h = \frac{h'T^*}{7.57 P^*} \quad (5)$$

The NASA TN D-8401 document provided us with the information necessary to compute the absolute humidity,  $h'$ , which is needed to compute the molecular absorption losses. The absolute humidity is typically found using data tables for relative humidity, dew point, and absolute humidity. To make the code independent from these data tables the calculation proposed by the NASA TN D-8401 document would be used in place of the tables. Equation (6) shows the absolute humidity as a function of temperature and dew point. The code requires the ambient temperature and dew point temperature along with the ambient pressure to be input in order to make the overall calculations. The constants for Eq. (6) are given by Table 1. The appropriate constants are chosen depending on whether the ambient temperature is above or below the freezing point of water.

$$h' = H(T, D) = k(T + d)^{-1} 10^{[c+b/(D+d)](D + d)^a} \quad (6)$$

	Over water <sup>1</sup>		Over ice <sup>2</sup>	
	SI	U.S. Customary Units	SI	U.S. Customary Units
a	-4.9283	-4.9283	-0.32286	-0.32286
b	-2937.4	-5287.32	-2705.21	-4869.38
c	23.5518	23.2801	11.4816	10.0343
d	273	459.4	273	459.4
<sup>3</sup> f	6.600 × 10 <sup>-4</sup>	3.595 × 10 <sup>-4</sup>	6.600 × 10 <sup>-4</sup>	3.595 × 10 <sup>-4</sup>
<sup>3</sup> g	7.570 × 10 <sup>-7</sup>	2.336 × 10 <sup>-7</sup>	7.570 × 10 <sup>-7</sup>	2.336 × 10 <sup>-7</sup>
k	0.21668	0.82455	0.21668	0.82455
a <sub>1</sub>	-4.9283	-4.9283	-4.9283	-4.9283
b <sub>1</sub>	-2937.4	-5287.32	-2937.4	-5287.32
c <sub>1</sub>	23.5518	23.2801	23.5518	23.2801

<sup>1</sup>Use Over water section for forms containing T' or D above freezing.

<sup>2</sup>Use Over ice section for forms containing T' or D at or below freezing.

<sup>3</sup>Constants must be multiplied by 0.882 if wet bulb is covered by thin layer of ice.

**Table 1. Constants Used for Absolute Humidity Calculation [5]**

### VIII. Verification and Validation of ALGPS

Once the ALGPS code was completed, two test cases were defined to verify that the MathCad and FORTRAN code predictions could be replicated while at the same time validate ALGPS by comparing its predictions to actual data from rocket engine tests.

#### A. Case I: Near field LOX/ RP engine on a Water Cooled Deflector

The first test case was a 400,000 lbf class, LOX/RP engine mounted on a water-cooled deflector, where the deflector did not have sidewalls. Since the point of interest is in the near field region, only the MathCad code results

will be compared to the ALGPS predictions. Figure 10 gives a qualitative depiction of the engine mounted above the deflector and the relative location of the microphone. To begin the prediction, information about the engine and test configuration is provided as input to the code. Table 2 shows normalized values that were used for the first test case.

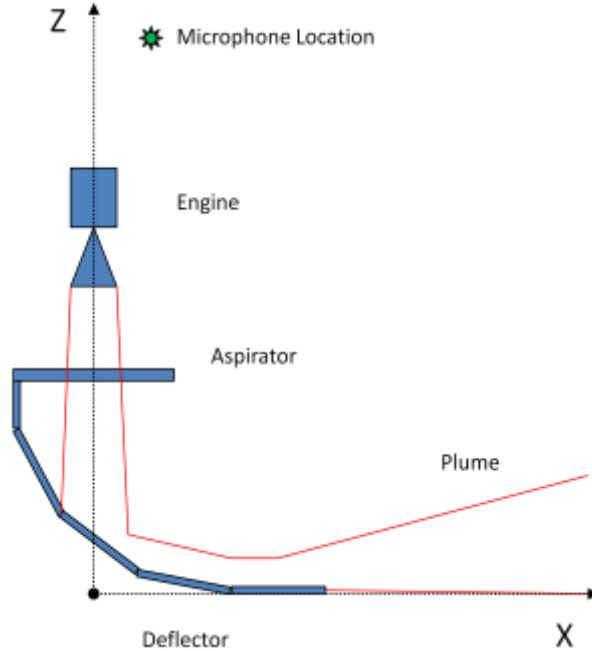


Figure 10. Case I Test Configuration

Engine/ Facility Configuration	
Thrust Class of Engine (klbf)	400
Fully Expanded Nozzle Exit Mach Number	3.4
$U_e/D_e$ (Hz)	1982
Number of Nozzles	1
Deflector Type	Open J-Deflector
Modeling Parameter Selection	
Acoustic Efficiency	0.425%
Acoustic Propagation	Hemispherical(ground plane present)
Source Allocation Method #1	
Velocity Acoustic Type (spectra)	2
Directivity Index Type	1
Points of Interest	
X/D, Y/D, Z/D	1.9, 0.0, 12.2

Table 2. Case I Input Information

The test case was modeled using both the first and second source allocation methods for comparative purposes. Table 3 displays the results that were obtained for both prediction methods. As indicated in Table 3 for the first

source allocation method, ALGPS was able to replicate the same OSPL values as the MathCad code. Also, Fig. 11 shows their spectra to be almost identical. While the first source allocation method provided a reasonable prediction of the acoustic spectra, it did so in an ad-hoc manner. The current version of the code does not allow for the deflected plume shape to be accounted for when using the first source allocation method. Rather, the plume had to be treated as an un-deflected straight plume with some ad-hoc corrections on “apparent” source location. The un-deflected plume was arbitrarily placed at the exit of the deflector.

Figure 11 also shows that the second source allocation method predictions were higher for the mid-frequency range compared to the first source allocation method. However, the roll off for the high and low frequency were in excellent agreement with the actual data shown in black. The authors believe that the differences between the spectrums in Fig. 11 were due to the aspirator shielding the acoustics that was located between the microphone and the plume, and was also due to the effects of water cooling which was not accounted for in any of the predictions. As of this date, ALGPS does not have the capability to account for acoustic shielding or water cooling. However, one important fact that should be noted is that the second source allocation method provided a conservative prediction and did not require ad-hoc assumptions of plume shape. In the future, the ALGPS code will be modified to account for the plume geometry when using the first source allocation method.

Parameter	MathCad SP-8072	ALGPS (Source Allocation Method #1)	ALGPS (Source Allocations Method #2)
Overall Acoustic Power (10 <sup>6</sup> Watts)	10.58	10.58	10.58
Overall Sound Power Level (dB, ref. 10 <sup>-12</sup> Watts)	190.25	190.25	190.25
<b>Overall Sound Pressure Levels</b>			
X/D, Y/D, Z/D=-2.3, 12.2, N/A	143.2	143.1	
X/D, Y/D, Z/D=1.9, 0.0, 12.2			149.5

**Table 3. Case I Results for MathCad Code and ALGPS (First and Second Source Allocation Method)**

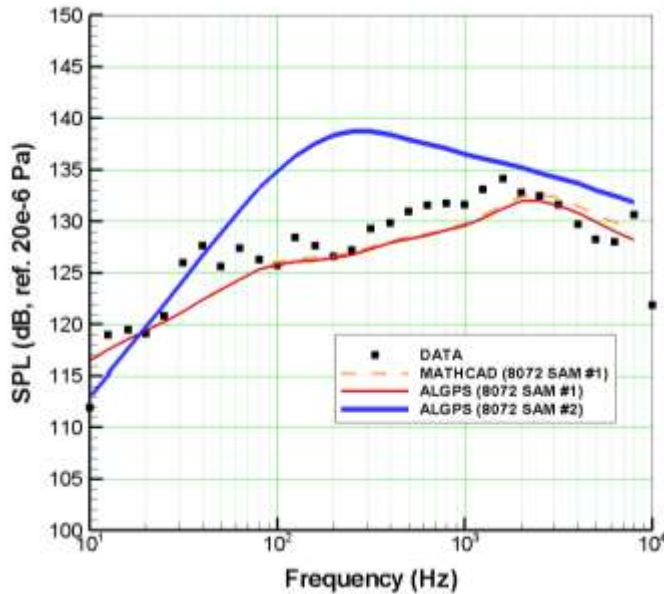


**Figure 11. Case I Sound Pressure Level Spectra**

**B. Case II: Mid/Far Field of LOX/RP Engine on Un-cooled Deflector**

For the second verification and validation case, the authors wanted to verify that ALGPS was able to reproduce the results for the FORTRAN code in the far-field acoustic region. The engine/deflector information provided as inputs to the code are provided in Table 4. Figure 12 shows the layout of the microphones with respect to the test stand for this test case. The microphones were placed in a region which probably would be classified as “mid-field” as the radial distance was slightly less than 100 diameters away. In this modeling effort, the authors used both the standard NASA SP-8072 directivity functions as well as the custom directivity index functions from the FORTRAN code.

Figure 13 shows the overall sound pressure level directivity for the microphones along the main arc (microphones 5, 2, 3, 4, and 8). The results for the point source method using the directivity index from the handbook, source allocation method one with the directivity index from the handbook, and the source allocation method one with custom directivity index data are compared to the FORTRAN code and the actual data. We can see that the first source allocation method with the custom directivity index is able to replicate the FORTRAN code with custom directivity index data and match the actual data very well. The spectrum for each of the methods were also compared to the actual data. The prediction methods provided consistent results with good comparison to the acoustic data for low to mid frequencies (<500 Hz). There were deviations seen between the actual data and the predictions towards the higher frequencies which were believed to be primarily due to acoustic shielding and the placement of the microphones. The deflector was below ground level which causes some of the noise to be blocked and also there is ground interference. This was proven in Fig. 15, when the data for microphone #7, which was placed on a nine foot pole, was compared to microphone #3 in the same location on the ground. The acoustic microphone data shows that the higher frequency acoustic data gets attenuated when the microphone is placed on the ground. The level of attenuation diminishes and the acoustic levels become more in agreement with the prediction curves when the microphones are elevated far above the ground level.

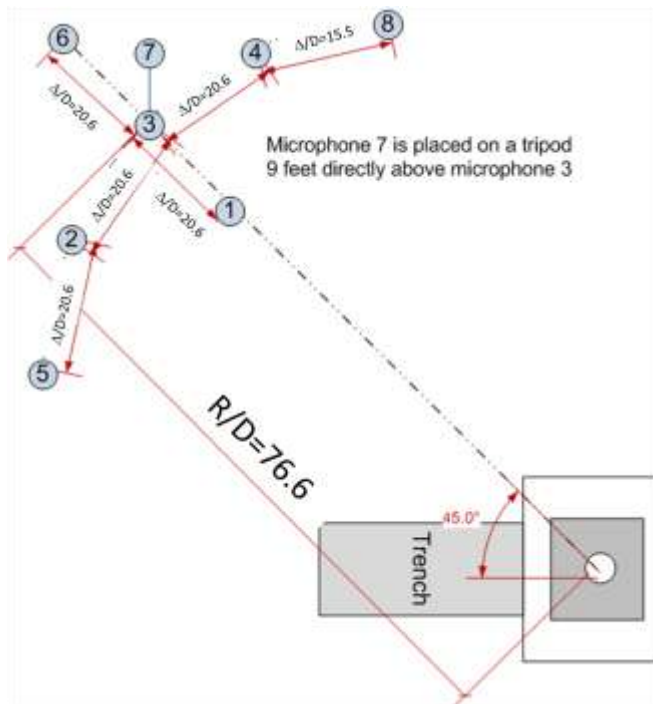


**Figure 12. Microphone Layout for Case II**

<b>Engine/ Facility Configuration</b>	
Thrust Class of Engine(klbf)	400
Fully Expanded Nozzle Exit Mach Number	3.4
$U_e/D_e$	1982
Number of Nozzles	1
Deflector Type	Closed J-Deflector
<b>Modeling Parameter Selection</b>	
Acoustic Efficiency	0.2%(best match to data)
Acoustic Propagation	Hemispherical(ground plane present)
Source Allocation Method #1	
Velocity Acoustic Type (spectra)	3
Directivity Index Type	2/3(custom)
<b>Points of Interest</b>	
X1/D, Y1/D, Z1/D	62.2, 62.2, 0.0
X2/D, Y2/D, Z2/D	89.7, 60.7, 0.0
X3/D, Y3/D, Z3/D	76.6, 76.6, 0.0
X4/D, Y4/D, Z4/D	60.7, 89.7, 0.0
X5/D, Y5/D, Z5/D	99.6, 42.6, 0.0
X6/D, Y6/D, Z6/D	91.2, 91.2, 0.0
X8/D, Y8/D, Z8/D	47.3, 97.4, 0.0

Table 4. Case II Input Information

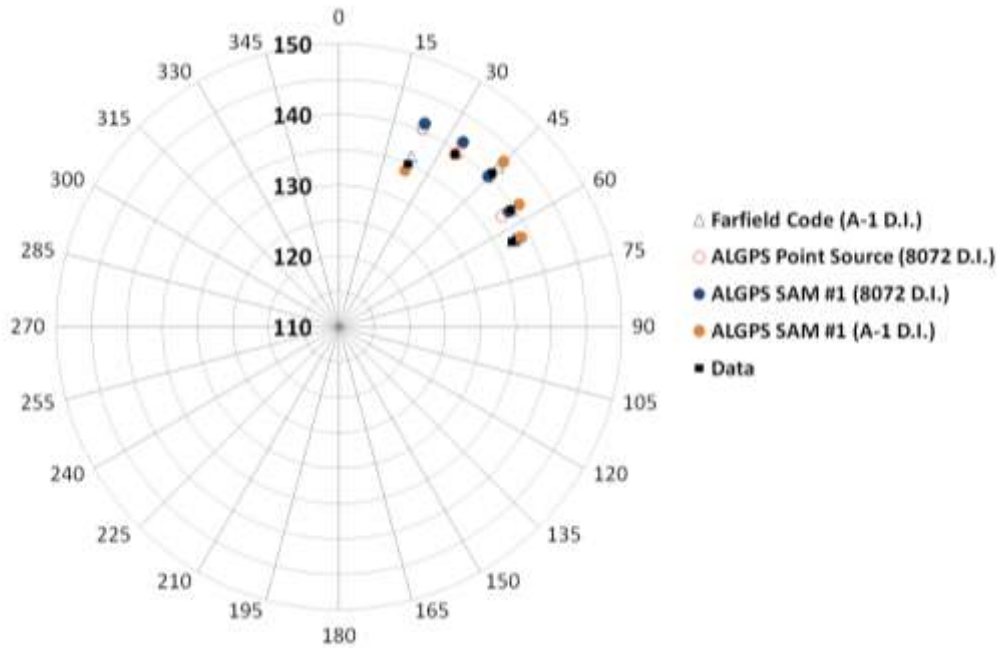


Figure 13. Case II OSPL Directivity

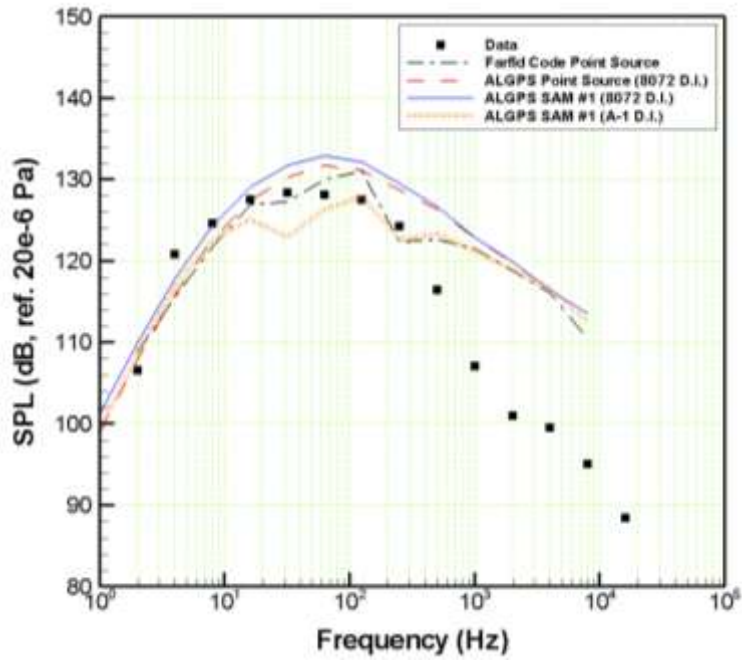


Figure 14. Case II Sound Pressure Level Spectra (15 deg. angle)

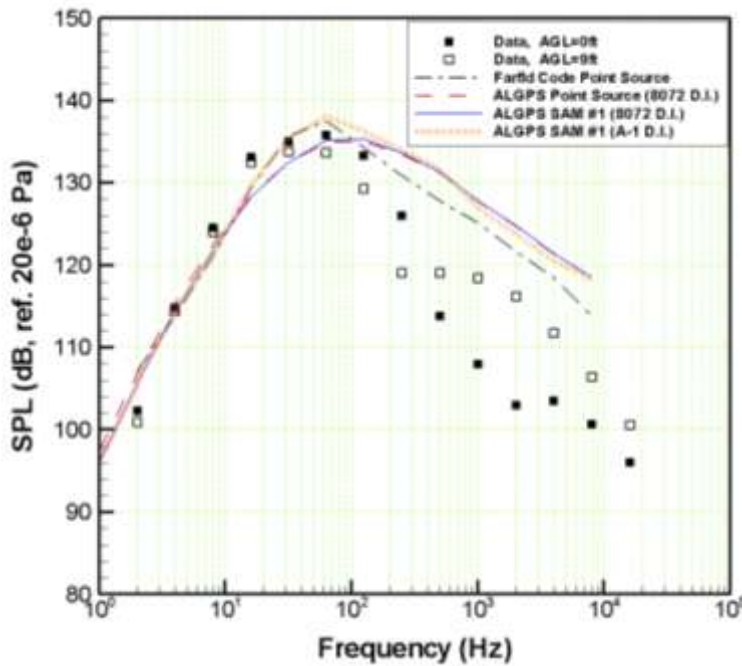


Figure 15. Case II Sound Pressure Level Spectra (45 deg. angle)

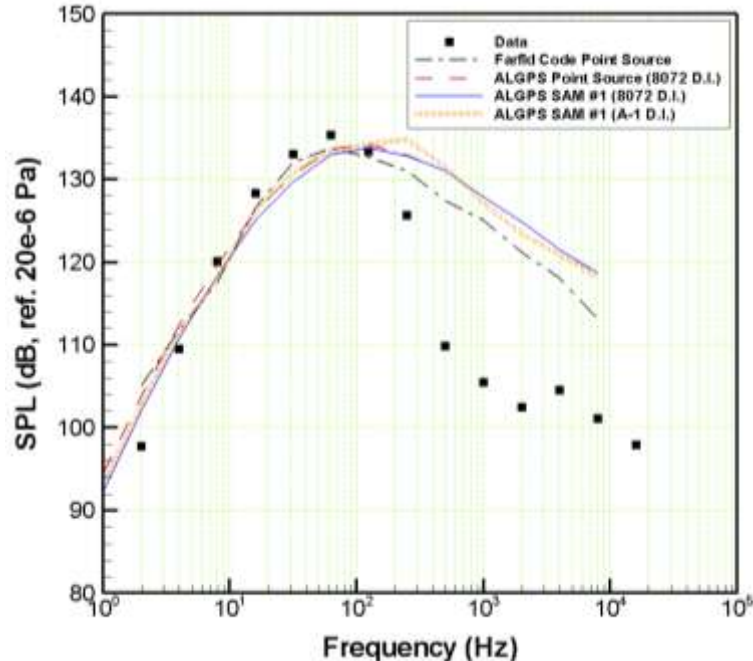


Figure 16. Case II Sound Pressure Level Spectra (60 deg. angle)

### IX. Conclusion

The new prediction tool was able to replicate the results from the previous prediction tools and reasonably matched the actual data for both near and far-field applications. Atmospheric attenuation functions were added to make the predictions more accurate in the far-field. The second source allocation method allowed us to make predictions without having to make idealizations of a free plume when the real testing configuration was a deflected plume. Based on this work, the ALGPS code can be now used to make future predictions at Stennis Space Center and will provide a common framework for implementing modeling improvements. Some additional functionality planned in the future includes accounting for excess attenuation corrections, wind effects, temperature inversions, and ground plane interference.

### Acknowledgments

Linamaria Perez thanks Daniel C. Allgood for serving as mentor and providing guidance in creating the prediction tool. The authors would also like to thank Richard Wear of NASA-Stennis Space Center, for providing assistance in obtaining the appropriate formulations for computing absolute humidity, which was needed for modeling atmospheric attenuation.

### References

- <sup>1</sup> Eldred, K.M., "Acoustic Loads Generated by the Propulsion System", NASA SP-8072, 1971.
- <sup>2</sup> Sutherland, L.C., "Sonic and Vibration Environments for Ground Facilities...a Design Manual", NAS8-11217, Huntsville, AL, 1968.
- <sup>3</sup> "Acoustic Energy Hazards", Hazards of Chemical Propellants handbook, AD 889763, CPIA/194, 1972.
- <sup>4</sup> Kinsler, L.E., Frey, A.R., Coppens, A.B., and Sanders, J.V., *Fundamentals of Acoustics*, 4<sup>th</sup> ed., John Wiley & Sons, Inc., Hoboken, NJ, 1976.
- <sup>5</sup> Parish, O.O, and Putnam, T. W., "Equations for the Determination of Humidity from Dewpoint and Psychrometric Data", NASA TN D-8401, Washington, D.C., 1977.
- <sup>6</sup> Haynes, J., and Kenny, J., "Modification to the NASA SP-8072 Distributed Source Method II for the Ares I Lift-off Environment Predictions", AIAA, 2009